# Sinogram noise reduction for low-dose CT by statistics-based nonlinear filters

Jing Wang*[1], Hongbing Lu[2], Tianfang Li[1], and Zhengrong Liang[1]

[1] Departments of Radiology and Physics and Astronomy, State University of New York, Stony Brook, NY 11794, USA
[2] Department of Biomedical Engineering/Computer Applications, Fourth Military Medical University, Xi'an, Shanxi 710032, China

## ABSTRACT

Low-dose CT (computed tomography) sinogram data have been shown to be signal-dependent with an analytical relationship between the sample mean and sample variance. Spatially-invariant low-pass linear filters, such as the Butterworth and Hanning filters, could not adequately handle the data noise and statistics-based nonlinear filters may be an alternative choice, in addition to other choices of minimizing cost functions on the noisy data. Anisotropic diffusion filter and nonlinear Gaussian filters chain (NLGC) are two well-known classes of nonlinear filters based on local statistics for the purpose of edge-preserving noise reduction. These two filters can utilize the noise properties of the low-dose CT sinogram for adaptive noise reduction, but can not incorporate signal correlative information for an optimal regularized solution. Our previously-developed Karhunen-Loève (KL) domain PWLS (penalized weighted least square) minimization considers the signal correlation via the KL strategy and seeks the PWLS cost function minimization for an optimal regularized solution for each KL component, i.e., adaptive to the KL components. This work compared the nonlinear filters with the KL-PWLS framework for low-dose CT application. Furthermore, we investigated the nonlinear filters for post KL-PWLS noise treatment in the sinogram space, where the filters were applied after ramp operation on the KL-PWLS treated sinogram data prior to backprojection operation (for image reconstruction). By both computer simulation and experimental low-dose CT data, the nonlinear filters could not outperform the KL-PWLS framework. The gain of post KL-PWLS edge-preserving noise filtering in the sinogram space is not significant, even the noise has been modulated by the ramp operation.

**Keywords:** low-dose CT, sinogram noise reduction, statistics-based nonlinear filters, streak artifacts, KL-PWLS

## 1. INTRODUCTION

Low-dose CT (computed tomography) imaging is clinically desired and has been under progress in the last decade [1]. Recently statistical modeling and iterative image reconstruction has shown good results [2]. We have been investigating an alternative approach which treats the low-dose CT data noise in sinogram space for the Radon transform and inverts the transform by the well-established FBP (filtered backprojection) for image reconstruction [3-8]. By repeated phantom experiments, the low-dose (or mA) CT sinogram data were found to follow approximately a Gaussian distribution with a nonlinear dependence between the sample mean and sample variance, i.e., the noise is signal-dependent [3]. The sample mean and variance dependence can be described by an analytical formula [3, 6, 7]. The noise properties of signal-dependence with a determined relationship between the mean and variance were modeled into a PWLS (penalized weighted least square) cost function, and the cost function was minimized iteratively in the sinogram space, followed by FBP image reconstruction with very good results [7, 8]. Utilizing Karhunen-Loève (KL) transform to incorporate signal correlation for the PWLS minimization adaptive to each KL component was explored in [4]. Further investigation by applying edge-preserving filters on the reconstructed low-dose CT images after the KL-PWLS noise treatment was performed with excellent results in [5]. This work aims to answer two questions along our research track [3-8]: (1) how do the statistics-based nonlinear filters perform for this low-dose CT application with comparison to our KL-PWLS nonlinear adaptive noise filtering? And (2) can edge-preserving filters improve the results after the ramp amplifying operation on the residue noise after the KL-PWLS operation prior to backprojection

* Correspondence: Email: jingwang@mil.sunysb.edu; Phone: (631) 444 7921; Fax: (631) 444 6450.



Medical Imaging 2005: Image Processing, edited by J. Michael Fitzpatrick, Joseph M. Reinhardt, Proc. of SPIE Vol. 5747 (SPIE, Bellingham, WA, 2005)
1605-7422/05/$15 · doi: 10.1117/12.595662

operation for image reconstruction? Two nonlinear edge-preserving filters below were investigated in this work, which are based on local statistics and fully utilize the low-dose CT noise properties.

### 1.1 Anisotropic diffusion filter

The idea of anisotropic diffusion filter was first described by Perona and Malik [9] to detect edges in multiscale space. The diffusive process is suppressed or stopped at boundaries where the diffusion strength is controlled by the gradient of image intensity. Anisotropic diffusion filter has become very popular and has been proven to be effective for noise reduction and edge preservation in medical imaging [10, 11]. Gerig *et al.* [10] applied it to enhance the MR (magnetic resonance) images and Demirkaya [11] used it to reduce noise and image artifacts in CT images. However, as pointed out by Saha and Udupa [12], one important drawback of this approach is that it does not provide image-dependent guidance for selecting an optimum gradient magnitude. Therefore, many improved anisotropic diffusion filter algorithms have been proposed to overcome those limitations. Saha and Udupa [12] proposed a scale-based diffusive filtering algorithm using local scale information to control the degree of smoothing for different regions in the image. Liang and Wang [13] proposed a local scale-controlled piecewise linear diffusion filter for selective smoothing and edge detection.

### 1.2 Nonlinear Gaussian filters chain

The nonlinear Gaussian filters chain (NLGC) is another class of edge-preserving filters [14-16]. It is a process which reduces noise in images while tries to keep the coarser structures in images. The image passes a chain of nonlinear filters which are derived from Gaussian filters. The NLGC has several important advantages for noise reduction. It is numerically robust (choice of the parameters is not critical). It is much faster than robust statistics estimation smoothing. A chain of three to five filters with suitable parameters is enough to differentiate random noise from intrinsic information (structure) in an image.

## 2. METHODS

### 2.1 Noise model

Our previous analyses [3, 6, 7] indicate that the calibrated projection data of low-dose CT follow approximately a Gaussian distribution with an associated relationship between the data sample mean and variance which can be described by the following analytical formula:

$$\sigma_i^2 = f_i \times \exp(\rho_i / S) \tag{1}$$

where $\rho_i$ is the mean and $\sigma_i^2$ is the variance of the projection data at detector channel or bin $i$, $S$ is a scaling parameter and $f_i$ is a parameter adaptive to different detector channels or bins.

### 2.2 Modified anisotropic diffusion filter

Mathematically, the anisotropic diffusion equation for a two-dimensional (2D) image can be formulated as [9]:

$$\frac{\partial I(x,y,t)}{\partial t} = div(c(x,y,t)\nabla I(x,y,t)) \tag{2}$$

where *div* represents the divergence operator, $\nabla$ represents the gradient operator, $I(x,y,t)$ is the image intensity at time step $t$, and $c(x,y,t)$ is the diffusion coefficient that controls the strength of the diffusion process. The diffusion coefficient is a monotonically decreasing function of the gradient magnitude of image intensity. It equals to one when the gradient of image intensity is zero and becomes zero as the gradient approaches to infinity. This property of the diffusion coefficient will lead to a diffusion process, which mainly takes place in the interior of a region while the boundaries remain the same. In this paper, we adapt the following diffusion coefficient function that was proposed by Perona and Malik [9]:

$$c(x,y,t) = \exp(-(\frac{|\nabla I(x,y,t)|}{K})^2). \tag{3}$$

Choosing the four-nearest neighbors, the discrete formula of their algorithm [9] can be expressed as:

$$I_{x,y}^{t+1} = I_{x,y}^{t} + \lambda \sum_{n=1}^{4} c_n \bullet \nabla_n I \tag{4}$$

where $0 \le \lambda \le 1/4$ is chosen to stabilize the numerical scheme and $n$ is the subscript to indicate the four nearest neighbors of pixel $(x, y)$.

In numerical implementation, three parameters need to be specified: the number of iterations, λ in equation (4) to control the diffusion speed, and parameter $K$ in equation (3) to estimate the noise level. Perona and Malik [9] proposed two methods to estimate the noise level parameter $K$: (1) $K$ was set empirically to some fixed value and (2) $K$ was set, at each iteration, to be the 90% value of the computed histogram of the absolute values of the gradient throughout the updated result. Both methods are spatially invariant and do not take the noise properties into account. This could lead to error for treatment of signal-dependent noise, such as the one existed in low-dose CT sinogram data [6, 7]. For an accurate estimate of the nonstationary parameter $K$, the noise property of low-dose CT sinogram was then used.

In 2D case, two neighboring pixels in each sinogram image are involved in computing the gradient of image intensity. It has been shown that the variance of the difference of two independent Gaussian random variables equals to the sum of the variances of these two random variables. Based on this relationship, we propose to estimate $K$ by the following formula:

$$K = \sigma_{x,y}^2 + \sigma_n^2 \tag{5}$$

where $n$ was defined before. Based on equation (5), the noise level parameter $K$ is spatially adaptive and the degree of diffusion process depends on the noise level of the image or sinogram in this application. A larger variance will lead to a higher degree of diffusion according to equations (3) and (5) and thus will make noise reduction more effective for low-dose CT sinogram as shown below.

### 2.3 Modified nonlinear Gaussian filters chain

In this study, we adapted a similar NLGC as that of Aurich and Weule [14] and, therefore, similar notations will be used throughout this paper. For an image with value $I(p)$ at pixel $p$, a nonlinear Gaussian filtering operation is defined by [14]:

$$G_{\sigma_x,\sigma_z} I(p) = I(p) + \eta \frac{1}{N_p} \sum_{q \in P} g_{\sigma_x}(\|q-p\|) g_{\sigma_z}(I(q)-I(p)) \cdot (I(q)-I(p)) \tag{6}$$

$$\text{with} \quad g_\sigma(t) = \exp(-\frac{t^2}{2\sigma^2}) \quad \text{and} \quad N_p = \sum_{q \in P} g_{\sigma_x}(\|q-p\|) g_{\sigma_z}(I(q)-I(p)) .$$

where $\sigma_x$ and $\sigma_z$ are smoothing parameters measuring the width of $g_{\sigma_x}$ and $g_{\sigma_z}$, respectively. Notation $P$ covers the neighborhood of pixel $p$ and $\eta$ is chosen to provide numerical stability of the approximation. For sufficient smoothing, several filtering steps with different parameters are usually performed. Formally it may be written by the form of:

$$G^{\sigma_{xn}\sigma_{zn}} \cdots G^{\sigma_{x1}\sigma_{z1}} I \tag{7}$$

A chain of three to five filters with suitable parameters is enough to differentiate random noise from intrinsic information (structure) in an image [15, 16]. Choosing a "robust scale" [14] for rejection of edges for each pair of the neighboring pixels $p$ and $q$ in terms of the population standard deviation $\sigma_{p,q}$, the smoothing parameter $\sigma_z$ above can be expressed as:

$$\sigma_{z_{p,q}} = \omega \cdot \sigma_{p,q} = \omega \cdot \sqrt{\sigma_p^2 + \sigma_q^2} \tag{8}$$

where notation $\omega$ is a normalization weight and can be determined by the filtering function; and $\sigma_p$ and $\sigma_q$ are the standard deviation of pixel $p$ and $q$, which can be determined by equation (1). Thus, the choice of parameter $\sigma_z$ is spatially variant and locally adaptive to the noise variation.

### 2.4 KL domain penalized weighted least-square minimization noise filter

Based on the noise properties of low-dose CT sinogram, we previously proposed KL-PWLS minimization to suppress the noise in low-dose CT projection images. In the KL-PWLS filtering scheme, the KL transform is first applied to account for the correlative information among the neighboring views of tomographic projections. Then for each KL component, PWLS criterion was used to estimate the ideal signal. FBP was employed to reconstruct CT image after inverse KL transform was applied on the smoothed KL components. The details of implementation of the KL-PWLS minimization filter can be found in [4]. Improvement of the KL-PWLS approach was observed as compared to the traditional spatially-invariant low-pass linear filters [4].

## 3. RESULTS

### 3.1 Comparison of the nonlinear edge-preserving filters and the KL-PWLS for sinogram noise reduction

Computer simulation studies were performed for the comparison purposes among different noise filtering methods using the 2D Shepp-Logan head phantom, see Figure 1. Table I lists the parameters of the ellipsoids (or objects) in the phantom of 2×2 unit array, which was scaled and digitized into an array size of 512×512 $mm^2$ (i.e., the pixel side size is 1 mm). A total of 984 fan-beam projections each of 888 bins were simulated for a 2π rotation. Each projection value along a ray through the phantom was computed based on the known densities and intersection lengths of the ray with the geometric shapes of the objects in the phantom. The detector arrays are on an arc concentric to the X-ray source with a distance of 949 mm and the detector cell spacing is 1.0239 mm. The distance of X-ray source to the center of rotation was 408 mm. All the 1D projections were collected together as a sinogram of 888×984 array size. After the ideal or noise-free sinogram was generated, a signal-dependent Gaussian noise was added according to equation (1). Figure 1(a) shows the standard FBP reconstruction (with the ramp at the cutoff of Nyquist frequency) from the noise-free sinogram, demonstrating accurate reconstruction of the phantom. Figure 1(b) is a conventional FBP reconstruction from the noisy sinogram using the traditional low-pass Hanning noise filtering with an optimal cutoff frequency (i.e., 0.8 Nyquist frequency for this case), demonstrating a significant noise artifact.

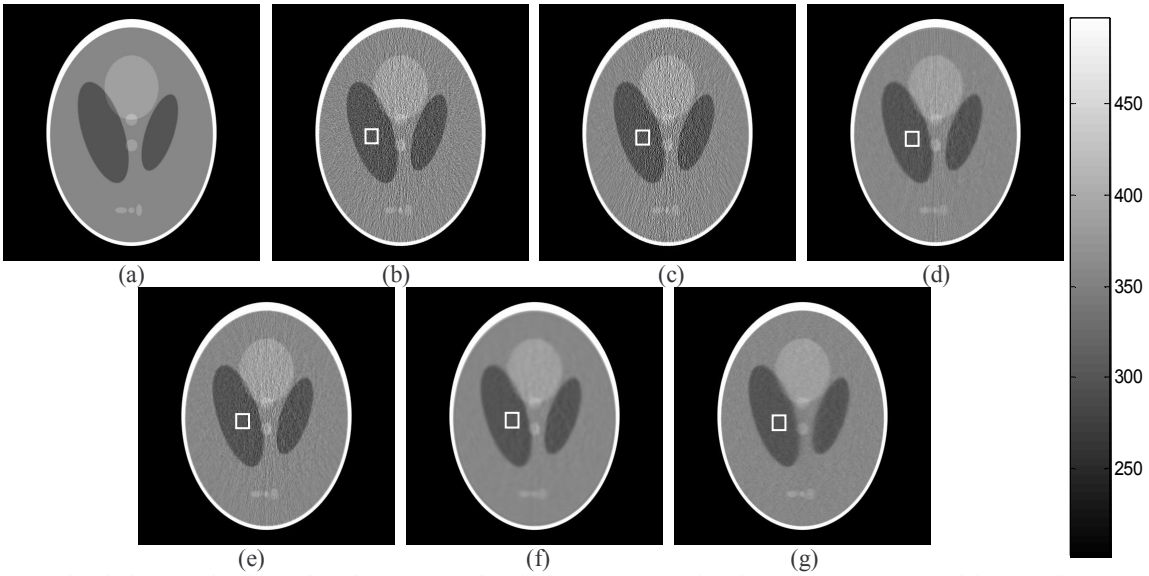


Figure 1: Simulation results from the Shepp-Logan head phantom: (a) noise free FBP reconstructed image; (b) FBP reconstructed image from noisy sinogram using conventional low-pass linear noise filtering; (c) FBP reconstructed image from noisy sinogram using the original anisotropic diffusion filter; (d) FBP reconstructed image from noisy sinogram using the modified anisotropic diffusion filter; (e) FBP noisy sinogram reconstructed image using the original NLGC filter; (f) FBP noisy sinogram reconstructed image using the modified NLGC filter; and (f) FBP reconstructed image from noisy sinogram using the KL-PWLS minimization.

#### 3.1.1 Modified anisotropic diffusion filtering results

A standard FBP reconstructed image from the filtered noisy sinogram by the original anisotropic diffusion filter is shown in Figure 1(c). Figure 1(d) shows a standard FBP reconstruction from the filtered noisy sinogram using the proposed anisotropic diffusion that uses equation (5) to estimate the noise level parameter $K$ in the diffusion process. In the diffusion procedure, the number of iterations was set to 20 and $\lambda$ was chosen as 0.1. The number of iterations and parameter $\lambda$ in the diffusion procedure were chosen based on error-trial for a visually appearing result for both the original and modified diffusion filters. Referring to Figure 1(b) and 1(c), it can be observed that both the original diffusion algorithm (due to its spatially invariant filtering) and the conventional low-pass spatially-invariant Hanning filter can not remove the noise-induced steak artifacts in the reconstructed CT images because they can not handle the signal-dependent noise in the low-dose CT sinogram properly. On the contrast, the modified statistics-based anisotropic diffusion filter takes the noise property of low-dose CT sinogram into account so that the steak artifacts in the reconstructed image can be removed efficiently.

TABLE I
PARAMETERS OF THE SHEPP-LOGAN HEAD PHANTOM

| Coordinates of center | Axis Lengths | Rotation angles | Intensity |
|---|---|---|---|
| (0.0, 0.0, 0.0) | (0.69, 0.92, 0.9) | (0, 0) | 600 |
| (0.0, -0.0184, 0.0) | (0.6624, 0.874, 0.88) | (0, 0) | -240 |
| (-0.22, 0.0, -0.25) | (0.41, 0.16, 0.21) | (-72, 0) | -60 |
| (0.22, 0.0, -0.25) | (0.31, 0.11, 0.22) | (72, 0) | -60 |
| (0.0, 0.35, -0.25) | (0.21, 0.25, 0.35) | (0, 0) | 30 |
| (0.0, 0.10, -0.25) | (0.046, 0.046, 0.046) | (0, 0) | 30 |
| (0.0, -0.10, -0.25) | (0.046, 0.046, 0.046) | (0, 0) | 30 |
| (-0.08, -0.605, -0.25) | (0.046, 0.023, 0.02) | (0, 0) | 30 |
| (0.06, -0.605, -0.25) | (0.046, 0.023, 0.02) | (90, 0) | 30 |
| (0.0, -0.605, -0.25) | (0.023, 0.023, 0.023) | (0, 0) | 30 |
| (0.0, -0.105, 0.625) | (0.056, 0.04, 0.10) | (90, 0) | 60 |
| (0.0, 0.10, 0.625) | (0.056, 0.056, 0.10) | (0, 0) | -60 |
| (0.0, -0.09, 0.0) | (0.055, 0.055, 0.055) | (0, 0) | 30 |
| (0.0, -0.09, 0.0137) | (0.039, 0.039, 0.039) | (0, 0) | 30 |
| (0.0, -0.09, 0.0238) | (0.0234, 0.0234, 0.0234) | (0, 0) | 30 |
| (0.0, -0.09, 0.0316) | (0.0156, 0.0156, 0.0156) | (0, 0) | 30 |

TABLE II
SNR FROM THE SHEPP-LOGAN HEAD PHANTOM STUDY

| Figure 1 | Mean | Stdv. | SNR |
|---|---|---|---|
| (b) | 301.4 | 35.4 | 8.4 |
| (c) | 301.9 | 40.3 | 7.5 |
| (d) | 300.6 | 9.4 | 32.1 |
| (e) | 300.5 | 8.1 | 37.1 |
| (f) | 300.7 | 5.8 | 51.8 |
| (g) | 300.8 | 4.0 | 75.1 |

TABLE III
SNR FROM THE 10 MA SHOULDER PHANTOM STUDY

| Figure 3 | Mean | Stdv. | SNR |
|---|---|---|---|
| (a) | 421.0 | 75.0 | 5.6 |
| (b) | 420.6 | 70.1 | 6.0 |
| (d) | 424.8 | 9.1 | 46.7 |
| (e) | 421.2 | 23.2 | 18.1 |
| (f) | 422.1 | 18.9 | 22.3 |
| (g) | 425.7 | 8.6 | 49.5 |

For more quantitative comparison, we calculated the signal-to-noise ratio (SNR) of a uniform area (marked with a square in Figure (1) in the reconstructed images to quantify the improvement of the modified anisotropic diffusion filter. The SNR is defined as the local mean divided by the local standard deviation (Stdv) of image densities in the selected area. Table II lists the Means, Stdvs, and SNRs of the uniform region in the reconstructed images of the Shepp-Logan head phantom. The SNR of the image reconstructed from the sinogram filtered by the modified anisotropic diffusion filter is much higher than that of the images reconstructed from the noisy sinogram filtered by the original anisotropic diffusion filter and the low-pass linear Hanning filter. These results also concur with the above observation.

We also show the effectiveness of the modified diffusion algorithm by a 10 mA low-dose CT noisy sinogram acquired from an anthropomorphic shoulder phantom. The sinogram of the phantom was acquired by a GE multi-slice spiral CT scanner with fan-beam curved detector arrays. The number of bins per view is 888 with 984 views evenly spanned on a circular orbit of 360°. The detector arrays are on an arc concentric to the X-ray source with a distance of 949 mm. The distance from the rotation center to the curved detector band is 408.075 mm. The detector cell spacing is 1.0239 mm.

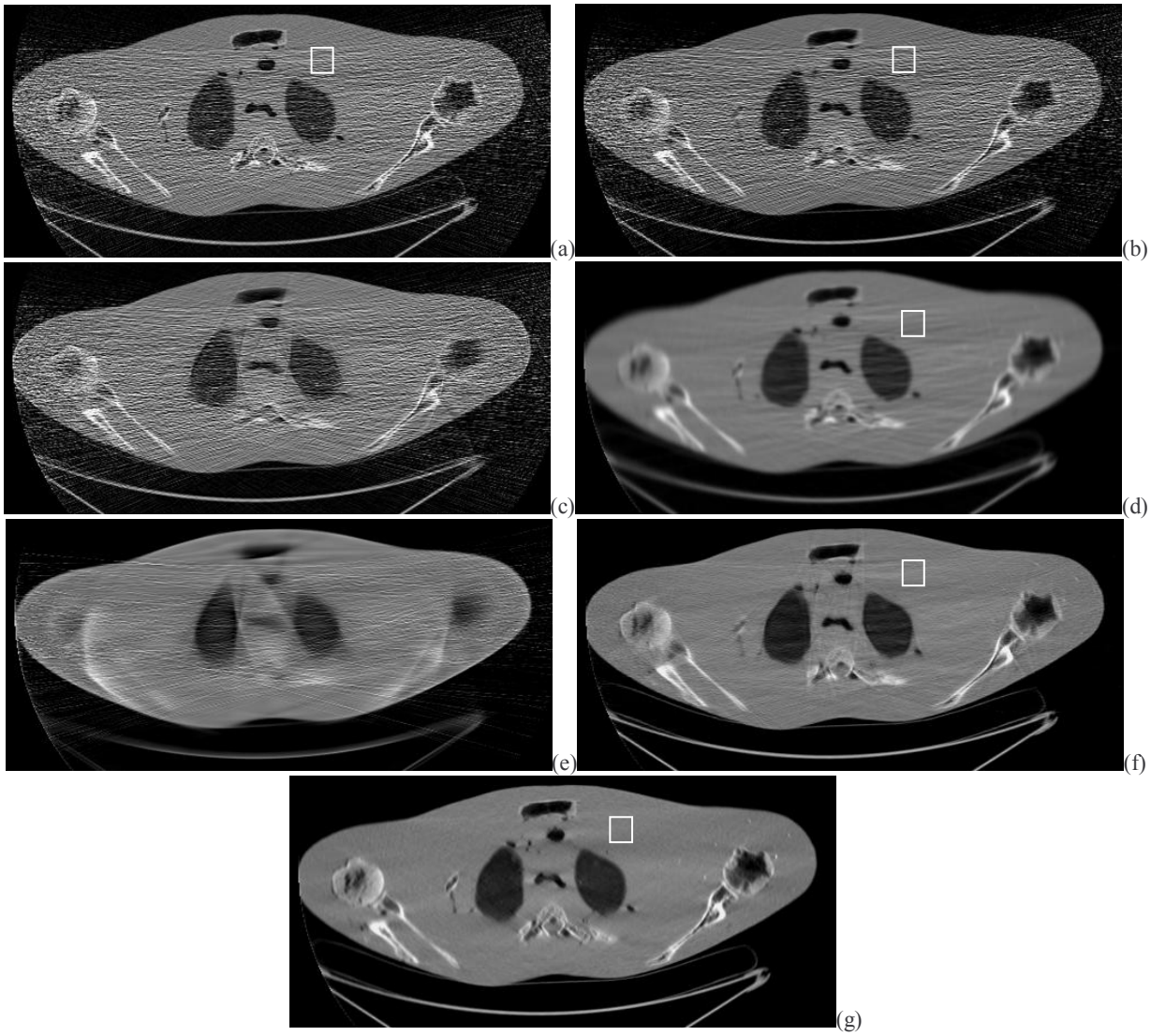


Figure 2: The CT images reconstructed by FBP from the 10 mA shoulder phantom data: (a) from the sinogram without noise reduction (i.e., the standard FBP reconstruction with ramp cutoff at the Nyquist frequency); (b) from the sinogram filtered by the original anisotropic diffusion filter with 20 iterations and $\lambda$=0.1 and (c) with 100 iterations and $\lambda$=0.2; (d) from the sinogram filtered by the modified statistics-based anisotropic diffusion filter with 20 iterations and $\lambda$=0.1; (e) from the sinogram filtered by the original NLGC; (f) from the sinogram filtered by the modified NLGC; and (f) from the KL-PWLS filtered sinogram.

The sinogram was first filtered by the anisotropic diffusion filter that uses equation (5) to estimate $K$ with 20 iterations and $\lambda$= 0.1. After the noise reduction, the CT image was reconstructed by the standard FBP (with the ramp cutoff at the Nyquist frequency), as shown in Figure 2(d). For comparison purposes, we also filtered the sinogram by the original anisotropic diffusion filter with the same parameters (number of iterations and $\lambda$), as shown in Figure 2(b), and

with different parameters, as shown in Figure 2(c). The CT image reconstructed by the standard FBP without noise filtering is shown in Figure 2(a). It can be clearly seen that the streak artifacts are effectively removed by the modified spatially-variant filtering of the non-stationary sinogram noise, while the streak artifacts still remain when the original spatially-invariant anisotropic diffusion filter was used. Table III lists the Means, Stdvs, and SNRs of the uniform regions indicated on the reconstructed images. It demonstrates that the modified anisotropic diffusion filter improves the SNR of the reconstructed image.

### 3.1.2 Modified nonlinear Gaussian filters chain results

Both the original and modified NLGC filters were tested by the Shepp-Logan head phantom simulations and the shoulder phantom experiments. The result from the original NLGC is shown in Figure 1(e) and from the modified NLGC is shown in Figure 1 (f) for the simulation data. The result of 10 mA should phantom from the original NLGC is shown in Figure 2(e) and from the modified NLGC is shown in Figure 2(f). In a similar performance as the anisotropic diffusion filter did, the streak artifacts could not be suppressed even the smoothing parameters are so large that some small structures have be distorted by the original NLGC algorithm. Improvement of the modified NLGC over the original NLGC can be clearly observed, also see Tables II and III.

### 3.1.3 KL-PWLS minimization results

We have shown the improvement of the modified anisotropic diffusion and NLGC filters over their original ones using the noise properties of CT sinogram to estimate the noise level parameters in the diffusion/Gaussian processes. However, their goal is to perform edge-preserving smoothing, not to estimate the noise-free data. Our previously proposed KL-PWLS minimization [4] aims to find an optimal solution for the noise-free data. Their different performance for the task of noise reduction for low-dose CT application was investigated using the simulation and experimental data in this paper. Figures 1(g) and 2(g) show the CT images reconstructed from the KL-PWLS filtered sinograms of the Shepp-Logan head phantom and the 10 mA shoulder phantom, respectively. It can be observed that the structures in the results from the KL-PWLS filtered sinograms are well-preserved while streak artifacts are removed efficiently compared to both the edge-preserving nonlinear filters. The SNRs in Tables II and III further confirm the above observation quantitatively.

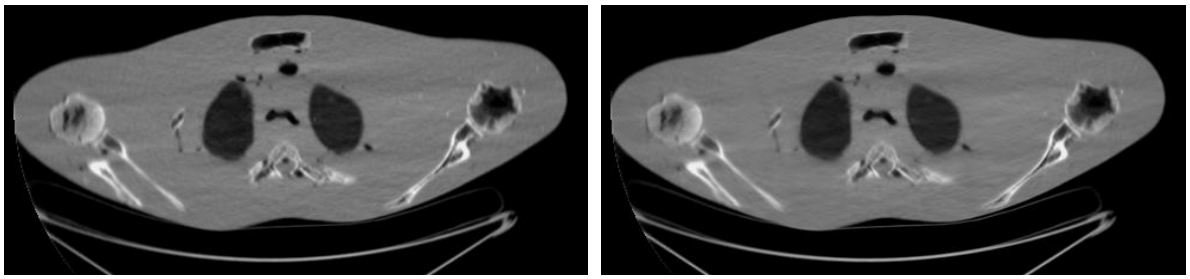

(a) (b)

Figure 3: (a) Result of anisotropic diffusion filter on ramp-filtered/amplified KL-PWLS-denoised sinogram; and (b) result of NLGC on ramp-filtered KL-PWLS denoised sinogram

### 3.2 Results of anisotropic diffusion filter and NLGC on ramp-filtered/amplified sinogram after KL-PWLS

Besides the noise treatment in the sinogram space above and in the reconstructed CT image domain [5], there is also another space to use the anisotropic diffusion filter or NLGC for noise reduction of low dose CT images. Zhong *et al* [17] tried to reduce the noise of cone-beam CT breast imaging by the use of wavelet-based denoising algorithms on the ramp-filtered projection images, followed by the Feldkamp algorithm for image reconstruction. It is known that in FBP reconstruction algorithm, the ramp filter will amplify high frequency noise due to its nature. To avoid amplifying the noise, we first applied the KL-PWLS minimization to treat the very noisy low-dose sinogram and then employed the anisotropic diffusion filter and NLGC on the ramp-filtered/amplified KL-PWLS denoised sinogram, prior to backprojection operation. Results of the 10 mA shoulder phantom experiment using the anisotropic diffusion filter and NLGC are shown in Figure 3(a) and 3(b) respectively. No significant improvement can be observed using the

anisotropic diffusion filter and NLGC on the ramp-filtered/amplified KL-PWLS denoised sinogram as compared to the result of using the KL-PWLS only. It is desirable to compare the KL-PWLS performance with the wavelet-based edge-preserving smoothing, such as the one used in reference [17], for the low-dose noisy sinogram.

## 4. DISCUSSION

Parameter of noise estimation plays an important role in the diffusion process for both the anisotropic diffusion filter and the NLGC. For images that are corrupted by signal-dependent noise, such as the low-dose CT sinogram, it is insufficient to determine the noise level parameter in the diffusion process using a global noise estimate. We have shown that the original anisotropic diffusion filter applying in sinogram space can not remove the streak artifacts in low-dose CT image. Even by choosing different number of iterations and different values for parameter $\lambda$, we were not able to obtain a comparable result to that treated by the modified non-stationary anisotropic diffusion filter. An example of 100 iterations with $\lambda$=0.2 for the original anisotropic diffusion filter is shown in Figure 2(c). It can be observed that the streak artifacts still present in the CT image while the structures of the image have been somewhat distorted. This simple experiment clearly demonstrates the importance of estimating the noise level parameter $K$. False estimation of $K$ cannot be compensated by the change of the number of iterations and value of $\lambda$. Similar results can be observed for NLGC as shown in Figure 2(e). Relatively accurate estimation for the noise level of each pixel based on noise statistics is necessary to obtain good result for both the anisotropic diffusion filter and NLGC algorithm. The modified filters are two examples of such necessary choice.

Although the original anisotropic diffusion filter and NLGC has been proven to be useful for noise reduction in medical images, it is not appropriate to apply these filters directly on the reconstructed low-dose CT images that contain the steak artifacts due to the low-dose nature (i.e., minimal X-ray exposure). The streak artifacts may be treated as edges of the reconstructed images in the diffusion process. Figures 4(a) and 4(b) show an example of applying the original anisotropic diffusion filter and NLGC directly to the standard FBP image of Figure 2(a). It can be clearly observed that the streak artifacts still present in the filtered images although the noise has been suppressed in the uniform region. Therefore sinogram filtering is necessary prior to image reconstruction.

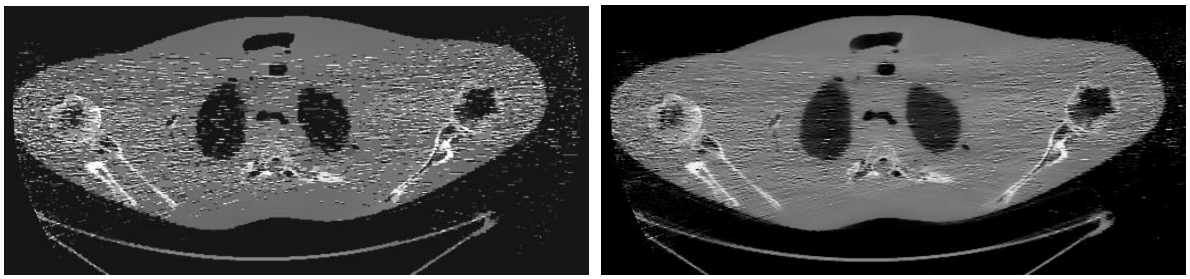

(a) (b)

Figure 4: (a) Result of filtering Figure 3(a) directly by the original anisotropic diffusion filter with $\lambda$=0.1 and 20 iterations; and (b) by the original NLGC with $\sigma_z$=100.

## 5. CONCLUSION

In this paper, we first modified the original anisotropic diffusion filter and NLGC scheme to incorporate the established noise properties of low-dose CT sinogram for a statistics-based noise reduction. The modification takes the statistical information of the data into account during the diffusive process. In the modified versions, the estimation of noise-level parameters is spatially adaptive, which is determined by the variance of pixels involved in the diffusion process. The improvement by the modified anisotropic diffusion filter and NLGC scheme is demonstrated by both computer simulations and phantom experiments mimicking the low-dose CT studies. Comparison study with our previously proposed KL-PWLS framework reveals that the KL-PWLS minimization provides better CT image quality in terms of noise suppression and structure preservation compared to the statistics-based nonlinear filters. This may be due to their different goals. The nonlinear diffusion filters aim only for edge-preserving noise reduction, while the KL-PWLS minimization seeks an optimal solution consistent to the measured data. Further study on a 10 mA shoulder phantom reveals that the gain by the edge-preserving noise filtering of the ramp-amplifying sinogram after the KL-PWLS

operation prior to backprojection operation is not significant. This implies that (1) the KL-PWLS minimization is effective for the noise reduction and the residue error after the KL-PWLS treatment is negligible (even after ramp amplification) and (2) edge-preserving noise smoothing is not an optimal choice for the low-dose CT noisy sinogram. Edge-preserving noise smoothing could not remove the noise-induced streak artifacts in low-dose CT images.

## ACKNOWLEDGEMENT

The authors wish to express their gratitude to Dr. J. Hsieh for providing the experimental phantom data. This work was supported in part by the NIH National Cancer Institute under Grant # CA82402 and the work of Dr. Lu was supported by the National Nature Science Foundation of China under Grant 30170278.

## REFERENCES

1. Otha W. Linton and Fred A. Mettler, Jr, "National conference on dose reduction in CT, with an emphasis on pediatric patients", *American Journal of Roentgenology* vol. 181 pp. 321-329, 2003.
2. Idris A. Elbakri and Jeffrey A. Fessler "Efficient and accurate likelihood for iterative image reconstruction in X-ray computed tomography", *SPIE Medical Imaging* vol. 5032, pp. 1839-1850, 2003.
3. Hongbing Lu, I-T Hsiao, Xiang Li, Jiang Hsieh, and Zhengrong Liang, "The analysis of noise properties in low-dose CT projections and its treatment by scale transformations", *Conf. Record of IEEE NSS and MIC*, 2001.
4. Hongbing Lu, Xiang Li, Ing-Tsung Hsiao, and Zhengrong Liang, "Analytical noise treatment for low-dose CT projection data by penalized weighted least-square smoothing in the K-L domain", *SPIE Medical Imaging* vol. 4682, pp. 146-152, 2002.
5. Hongbing Lu, Xiang Li, Lihong Li, Dongqing Chen, Yuxiang Xing, Mark Wax, Jiang Hsieh, and Zhongrong Liang, "Adaptive noise reduction toward low-dose computed tomography", *SPIE Medical Imaging* vol. 5030 pp. 759-766, 2003.
6. Tiangfang Li, Xiang Li, Yuxiang Xing, Hongbing Lu, Jiangxie Hsieh, and Zhongrong Liang, "A Strategy for Reduction of Streak Artifacts in Low-dose CT", *Conf Record IEEE NSS-MIC*, in CD-ROM, 2003.
7. Tianfang Li, Jing Wang, Junhai Wen, Xiang Li, Hongbing Lu, Jiang Hsieh, and Zhengrong Liang, "SNR-weighted sinogram smoothing with improved noise-resolution properties for low-dose X-ray computed tomography", *SPIE Medical Imaging* vol. 5370, pp. 2058-2066, 2004.
8. Tiangfang Li, Xiang Li, Jing Wang, Junhai Wen, Hongbing Lu, Jiang Hsieh, and Zhengrong Liang, "Nonlinear Sinogram Smoothing for Low-dose X-ray CT", *IEEE Transactions on Nuclear Science*, vol.51, no.4, 2505-2513, 2004.
9. Pietro Perona and Jitendra Malik, "Scale-space and edge detection using anisotropic diffusion", *IEEE Trans. Pattern Anal. Machine Intell.*, vol. 12, pp. 629-639, July 1990.
10. Guido Gerig, Olaf Kübler, Ron Kikinis, and Ferenc Jolesz, "Nonlinear anisotropic filtering of MRI data", *IEEE Trans. Med. Imaging*, vol. 11, pp. 221-232, June 1992.
11. Omer Demirkaya, "Reduction of noise and image artifacts in computed tomography by nonlinear filtration of the projection images", *SPIE Med. Imaging*, vol. 4322, pp. 917-923, 2001.
12. Punam Saha and Jayaram Udupa, "Scale-based diffusive image filtering preserving boundary sharpness and fine structures", *IEEE Trans. Med. Imaging*, vol. 20, pp. 1140-1154, November 2001.
13. Ping Liang and YF Wang, "Local scale controlled anisotropic diffusion with local noise estimate for image smoothing and edge detection", *Proc. Int. Conf. Computer Vision, Bombay*, India, pp. 193-200, 1998.
14. V Aurich and J Weule, "Non-linear Gaussian filters performing edge preserving diffusion", in *Proceedings 17. DAGM Symposium über Mustererkennung*, pp. 538-545, Springer, 1995.
15. CK Chu, IK Glad, F Godtliebsen, and *et al*, Edge-preserving smoothers for image processing, *J. of the American Statistical Association*, vol. 93, No. 442, pp. 526-541, 1998.
16. G Winkler, V Aurich, K Hahn, and *et al*, Noise Reduction in Images: Some Recent Edge-Preserving Methods, *Pattern Recognition and Image Analysis*, vol. 9, pp. 749-766, 1999.
17. Junmei Zhong, Ruola Ning, and David Conover, "Image denoising based on multiscale singularity detection for cone beam CT breast imaging", *IEEE Trans. Med. Imaging*, vol. 23, pp. 696-703, June, 2004.